International Journal of Engineering, Science and Mathematics
Vol. 6 Issue 6, October 2017,
ISSN: 2320-0294 Impact Factor: 6.765
Journal Homepage: http://www.ijesm.co.in, Email: ijesmj@gmail.com Double-Blind Peer Reviewed
Refereed Open Access International Journal - Included in the International Serial Directories Indexed & Listed at: Ulrich's Periodicals Directory ©, U.S.A., Open J-Gage as well as in Cabell's Directories of Publishing Opportunities, U.S.A

Coal Fly Ash consumption for sustainable environment management: Crystallization kinetics of mesoporous molecular sieve MCM-41

Shubhangi Atkare[1],
Dr. N.A. Kedar[2],
Dr.Manish Deshpande[3]

Dept. of Chemistry Dayanand Science College, Latur, Pin: 413512
Dept. of Physics N.S.B. College, Nanded, Pin: 431601

ABSTRACT:

We report ecological synthesis of mesoporous molecular sieves of M41S family using coal fly ash (CFA) available in ample as the thermal power station waste during electricity generation. This contributes to the green synthesis of MCM-41 at a cheaper production cost. Coal fly ash was used to synthesize MCM-41 by alkali fusion followed by hydro-thermal treatment and was characterized using various techniques viz. XRD, SEM, FTIR, TGA-DTG, N_2-sorption for surface area measurement etc. The synthesis and history dependent parameters were optimized to obtain highly crystalline phase of MCM-41. During the synthesis crystallization kinetics was studied. The highly crystalline nature and well ordered phase was obtained at 120^0C with utmost BET surface area 1053m^2/g with high purity. The activation energy of crystallization kinetics was found to be 160.31 kJ/mole.

Keywords*: Coal fly ash; MCM-41; hydrothermal synthesis parameter, Activation energy.*

1. INTRODUCTION

Hazardous wastes are generated annually throughout the world by all industries and their disposal poses major challenges of serious environmental problems[1-4] and health risks. In the recent years, there has been a growing interest to find creative ways not only to reduce natural waste and industrial hazard to overcome environmental pollution but also its effective utilization. As we know that, coal plays an increasingly important role to meet the ever-growing demand for energy. Coal-fired thermal power plants account for 57 % of the total electricity generation in India and will remain the mainstay to meet the additional capacity for upcoming requirements[5-8]. In the process of electric power generation using coal, about 120 million tones (mt) of fly ash is produced annually

International Journal of Engineering, Science and Mathematics
Vol. 6 Issue 6, October 2017,
ISSN: 2320-0294 Impact Factor: 6.765
Journal Homepage: http://www.ijesm.co.in, Email: ijesmj@gmail.com Double-Blind Peer Reviewed
Refereed Open Access International Journal - Included in the International Serial Directories Indexed & Listed at: Ulrich's Periodicals Directory ©, U.S.A., Open J-Gage as well as in Cabell's Directories of Publishing Opportunities, U.S.A

in India alone with more than 75000 hectares of land being occupied by ash ponds, thus causing severe environmental harms. Of the total 2,78,180 mt of coal deposits in India, approximately 2,76,810mt comes from the Gondwana stratigraphic horizon[9].

Chandrapur and Parali (Vz), are India's major thermal power stations in Maharashtra State. They are the biggest consumers of coal per annum for electric power generation process. Upon combustion of coal during electric power generation process, the coal forms fly ash particles. These fly ash particles create serious ecological problems and disposal of such a massive quantity of ash has become a vital issue. CFA is mainly composed of some oxides i.e. SiO_2 and Al_2O_3 which remain even after the combustion of the coal.

In 1992, scientist at Mobil Oil Corporation[10] discovered new family (M41S) of mesoporous materials[11], (MCM-41, MCM-48 etc.). MCM-41[12] possesses hexagonal and MCM-48 possesses lamellar arrangement of mono dimensional molecular sieves having fairly uniform pores with pore diameter[13] of 20-100Å.

Our research endeavors the use of no-cost raw materials such as industrial waste CFA collected from the Chandrapur and Parali (Vz) Thermal Power Stations Maharashtra (India). The reasons for choosing these sources for our further investigations are: 1) They add value; reduce the cost and effective utilization to protect the environment.2) Their potential application in synthesis of highly useful porous materials.3) Their potential application in water purification technology, as industrial catalyst, supporting materials, exchanger, molecular sieves etc[14].

2. MATERIALS AND METHODS:

2.1 Pre treatment on CFA:

CFA obtained from Chandrapur and Parali TPS, was screened by sieve of 80-mesh size to eradicate the larger particles. The unburnt carbon along with other volatile materials present in CFA was removed by calcination at 800°C for 5h in muffle furnace. CFA was then treated with dilute hydrochloric acid to remove iron to a certain extent. An amorphous SiO_2 component in the CFA was used as Si-source for the further investigations.

2.2 Chemical Composition of Coal Fly Ash (CFA):

The Chemical composition of fly ash collected from Chandrapur and Parali (vz) was determined by X-ray fluorescence (XRF) and Atomic adsorption spectroscopy and obtained values are tabulated in Table:1

International Journal of Engineering, Science and Mathematics
Vol. 6 Issue 6, October 2017,
ISSN: 2320-0294 Impact Factor: 6.765
Journal Homepage: http://www.ijesm.co.in, Email: ijesmj@gmail.com
Double-Blind Peer Reviewed
Refereed Open Access International Journal - Included in the International Serial Directories Indexed & Listed at: Ulrich's Periodicals Directory ©, U.S.A., Open J-Gage as well as in Cabell's Directories of Publishing Opportunities, U.S.A

Table:1 Chemical analysis of CFA

Components	CFA Parali (vz)TPS	CFA Chandrapur TPS
Na_2O	0.23%	0.24%
Al_2O_3	18.18%	12.41%
SiO_2	69.12%	80.06%
K_2O	0.40%	0.56%
CaO	1.42%	1.06%
TiO_2	2.32%	1.28%
BaO	1.01%	0.98%
MgO	0.32%	0.19%
Fe_2O_3	7.0%	3.22%
Surface area	2.9(m^2/g)	2.68(m^2/g)
Mean particle size	24.90µm	24.93µm

From the chemical analysis of CFA (Table:1) obtained from Chandrapur TPS and Parali TPS, we came to know that CFA of Chandrapur TPS is more silicious, therefore we have decided to take it as a main Silica source.

2.3 Synthesis of MCM-41 from CFA in alkaline medium

The MCM-41phase was hydrothermally synthesized under the molar system

1.0SiO_2: 1.5NaOH: 0.008 (CTAB): 0.08 EA: 42H_2O.

at different temperatures starting from 30 to 160 ^{0}C for 4 hrs under stirring condition (300 rpm). After hydrothermal treatment the mixture was cooled and filtered till the effluent shows neutral pH. The collected cake was dried and calcined at different temperatures ranged from 450 to 800 ^{0}C at a ramp of 50^{0}C keeping heating rate of 1^{0}C/min for durations of calcination 4.5h.After cooling; the samples were characterized for the investigation of optimization. This synthesized material is further known as CFA-MCM-41.

3. RESULTS AND DISCUSSION

The collected fly ash was analyzed by XRD, SEM, FTIR techniques and also synthesized samples are characterized by techniques such as XRD, N_2-sorption, SEM, TGA/DTA, FTIR etc. to elucidate their structural features, pore architecture, morphology, thermal stability, surface area and activation energy during crystallization[15-16].

3.1 Mineralogical properties of CFA.

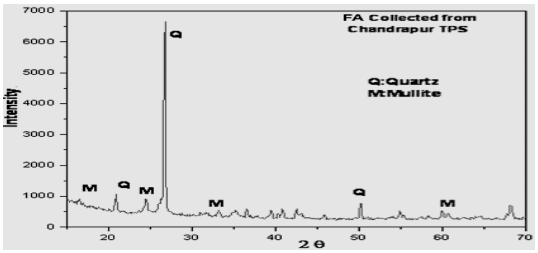

Fig.1XRD Pattern of treated CFA obtained from Chandrapur TPS

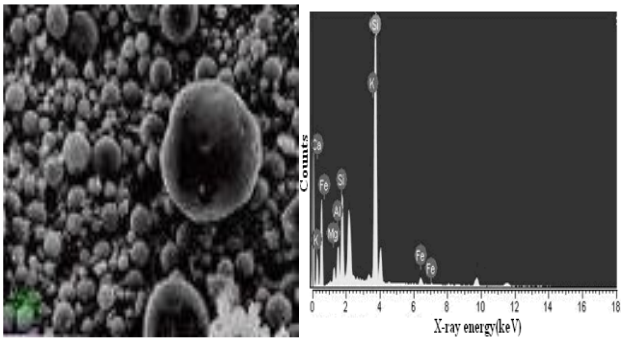

(A) (B)

Fig.2:(A, B) The scanning electron micrographs (SEM) of the treated CFA and EDS of CFA

International Journal of Engineering, Science and Mathematics
Vol. 6 Issue 6, October 2017,
ISSN: 2320-0294 Impact Factor: 6.765
Journal Homepage: http://www.ijesm.co.in, Email: ijesmj@gmail.com
Double-Blind Peer Reviewed
Refereed Open Access International Journal - Included in the International Serial Directories Indexed & Listed at: Ulrich's Periodicals Directory ©, U.S.A., Open J-Gage as well as in Cabell's Directories of Publishing Opportunities, U.S.A

3.2 XRD analysis of synthesized material

X-ray diffraction spectra which were scanned on an instrument MiniFlex-2 goniometer using a monochromatic Cu-Kα radiation (40 kV, 25mA) with a 0.02 step size and a 1.2 s step time with a wave length of 1.540A^0. From the XRD pattern shown in Fig.1, strong peaks of 2θ values at 22.7º, 26.9º, 27.06º, 50.66º and 68.96º exhibited the predominant crystalline phases of quartz (SiO_2 i.e. Q), intense peaks of 2θ values at 5.4º, 24.9º and 33.2º shows the presence of mullite (alumino-silicate i.e. M) phases. The XRD pattern of CFA also shows peak at 33.4º indicating the presence of calcite.

The scanning electron micrograph (SEM) of the treated CFA is depicted in Fig.2-A.The micrographs showed agglomerated[17] and irregularly shaped amorphous particles associated with aggregates of polycrystalline, amorphous and glassy material. As determined by EDS (Fig.2-B), the identified elements in the ash samples show strong concentrations of O, Al, Si, with lower levels of Na, Mg, K, Ca, Ti, and Fe.

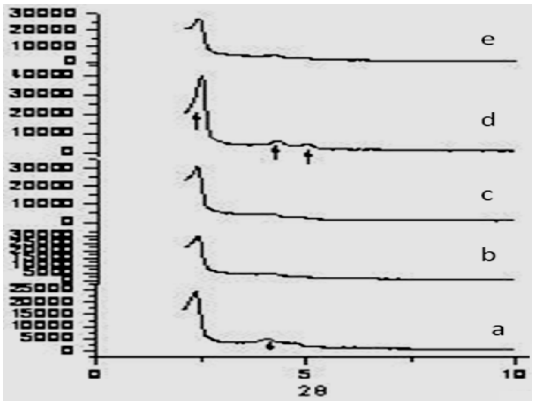

Fig.3:XRD patterns of calcined samples of CFA-MCM-41 synthesized at 30,70,100,130,160 ^{0}C (a-e)

The XRD pattern of CFA-MCM-41 synthesized at different hydrothermal temperatures and calcined at 550^{0}C for fixed duration of 4.5h are shown in Fig.3. The XRD pattern at 30^{0}C suggests that this material does not possess the well defined hexagonal arrays after calcinations as it shows only the (100) reflection prominently. It indicates that the maximum contraction of unit cells, which may be due to the poorly ordered arrangement of the mesopores. However, the long range order in hexagonal symmetry is started to develop from 70 to 130^{0}C hydrothermal temperature.

A significant increase in the intensities of these four peaks indexed at 100,110,200,210 indicates that an atomic reorganization occurs during the removal of the surfactant molecules in the calcination process. All these four reflections are well defined in the sample synthesized at 130^{0}C. This sample is treated as 100% crystalline sample. The unit cell parameter, percent crystallinity of all the samples were calculated and

International Journal of Engineering, Science and Mathematics
Vol. 6 Issue 6, October 2017,
ISSN: 2320-0294 Impact Factor: 6.765
Journal Homepage: http://www.ijesm.co.in, Email: ijesmj@gmail.com
Double-Blind Peer Reviewed
Refereed Open Access International Journal - Included in the International Serial Directories Indexed & Listed at: Ulrich's Periodicals Directory ©, U.S.A., Open J-Gage as well as in Cabell's Directories of Publishing Opportunities, U.S.A

represented in Table 2.

The percent crystallinity of the samples drawn at different synthesis temperatures in the crystallization kinetics was obtained by the following relation.

$$\% \text{ Crystallinity} = \frac{\text{Sum of the peak heights of unknown material} \times 100}{\text{Sum of peak heights of standard material}}$$

The obtained values of % crystallinity were further plotted as a function of temperature from which the gradient of crystallization has been evaluated. The percent conversion from amorphous to 100 % crystalline product of CFA-MCM-41 phase is shown in the Fig.4. The kinetic curve describing the increase in the crystallinity of the crystals with the synthesis temperature is nearly "S" shaped that depends on rate of conversion. This type of sigmoidal nature of crystallization curve indicates two distinct stages, namely an induction period and a crystal growth period. It is seen from the Fig.4 that up to 70^0C the rate of conversion of amorphous to crystallization of CFA-MCM-41 phase was initially slow and then it is increased sharply between 70^0C to 130^0C followed by subsequent slow down. Therefore, the rate of crystallization decreases as the process approaches to the completion indicated by constancy (100 %) in percent crystallization.

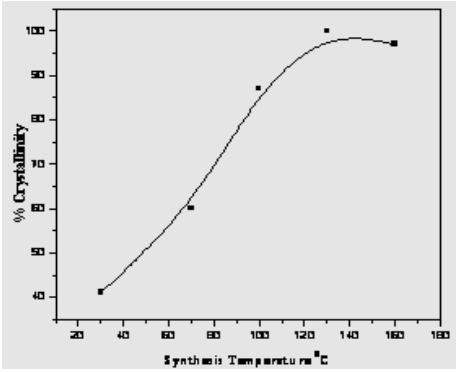

Fig.4 Kinetics of crystallization of CFA-MCM-41

The apparent activation energy for conversion was estimated from the slope of linear plot of ln K vs. (1/T) by applying the Arrhenius equation[18]

$$d \ln K / d(1/T) = E_{ac}/RT$$

Where, K is the rate of conversion, E_{ac} is the energy of crystallization/ conversion, R is the gas constant. By the application of Arrhenius equation, the apparent activation energy of conversion of aluminosilicate gel to 100 % crystalline CFA-MCM-41 phase was calculated and found to be 169.44 kJ/mole in the present crystallization system. However, with further increase in the temperature to160°C, the hexagonal phase changes to a lamellar one under the synthesis conditions.

3.3 BET surface area and pore volume of CFA-MCM-41

The obtained N_2-adsorption-desorption isotherms and corresponding BJH pore size distribution is shown Fig.5A, B. Further using

International Journal of Engineering, Science and Mathematics
Vol. 6 Issue 6, October 2017,
ISSN: 2320-0294 Impact Factor: 6.765
Journal Homepage: http://www.ijesm.co.in, Email: ijesmj@gmail.com Double-Blind Peer Reviewed
Refereed Open Access International Journal - Included in the International Serial Directories Indexed & Listed at: Ulrich's Periodicals Directory ©, U.S.A., Open J-Gage as well as in Cabell's Directories of Publishing Opportunities, U.S.A

these isotherms data, BET surface Area, respective pore diameter and volume were calculated. The calculated data is shown in following Table 2.

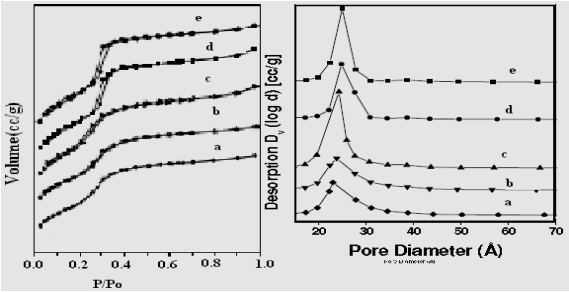

Fig. 5(A) N2 adsorption-desorption isotherms and (B) pore size distribution of CFA-MCM-41(a, b, c, d, e)

According to IUPAC classification, these isotherms of CFA-MCM-41 are of type IV[19], which is the characteristic of mesoporous material. The isotherms exhibit three stages. The first stage is a linear part almost going through the origin, which is due to monolayer adsorption of nitrogen on the walls of the mesopores ($p/p_0 < 0.2$). The second stage is characterized by a steep increase in adsorption (within the relative pressure p/p_0 range of 0.2-0.4) due to capillary condensation of N_2 in the pore channels. This part shows hysteresis.

In pore size distribution curve, narrow and sharp peak is observed in the diameter range 20-25 Å showing uniform pore size. The isotherms of the samples show small hysteresis loop in the lower pressure regions. The surface area (1276.6m^2/g) is an indication of well dispersion of active sites. The statistical data given in Table 2 reflects that, as the synthesis temperature increases from 70^0C to 130^0C the unit cell parameter marginally increases in samples. After 130^0C, d_{100} spacing reduces and accordingly unit cell parameter maintains the same trend indicating the cause of disturbing the well crystalline hexagonal array of the material. The surface area is increased with the increase in synthesis temperature from 30^0C to 130^0C due to the progressive formation of ordered mesophase silica. However, the surface area decreases with further increase in synthesis temperature due to silica pore shrinkage. This suggests that increasing the synthesis temperature can accelerate the silicate condensation on the silica wall, which subsequently thickens the silica framework.

International Journal of Engineering, Science and Mathematics
Vol. 6 Issue 6, October 2017,
ISSN: 2320-0294 Impact Factor: 6.765
Journal Homepage: http://www.ijesm.co.in, Email: ijesmj@gmail.com
Double-Blind Peer Reviewed
Refereed Open Access International Journal - Included in the International Serial Directories Indexed & Listed at: Ulrich's Periodicals Directory ©, U.S.A., Open J-Gage as well as in Cabell's Directories of Publishing Opportunities, U.S.A

Table 2. Effect of crystallization temperature on Structural and textural properties of CFA-MCM-41 calcined at 550^{0}C for 4.5h

Samples Name/synthesis Temperature in ^{0}C CFA-MCM-41	d_{100}	Unit cell parameter	S.A. (m^2/g)	Average pore diameter (Å)	Pore volume (ml/g)	Average wall thickness (Å)	% Crystallanity
(a)/30	33.43	38.78	684.04	30.87	0.478	7.91	41
(b)/70	33.97	39.41	785.13	27.53	0.575	11.88	60
(c)/100	35.78	41.51	1101.3	24.12	0.664	17.39	87
(d)/130	36.83	42.72	1276.6	17.53	0.701	25.19	100
(e)/160	35.19	40.82	889.94	28.41	0.532	12.41	97

3.4 FTIR-studies

The FTIR spectra of CFA-MCM-41(30, 70, 130, 160^{0}C) are illustrated in Fig.6. The broad band around 3500cm^{-1} is due to surface silanols and adsorbed water molecules which indicating the silica framework is hydrophilic. The disappearance of peak at 2922.9cm^{-1} and 2852.5cm^{-1} can be concluded that the calcination at 550^{0}C is complete. This indicates that the organic template has been removed completely due to calcination. Bands observed at 1234.3cm^{-1} and 1071.4cm^{-1}are characteristics peaks of asymmetric Si-O-Si stretching. Another characteristics peak is the symmetric Si-O-Si stretching observed at 785.9cm^{-1}. However, the peak at 2319.7cm^{-1} is prominently found to be changed due to the effect of synthesis temperature.

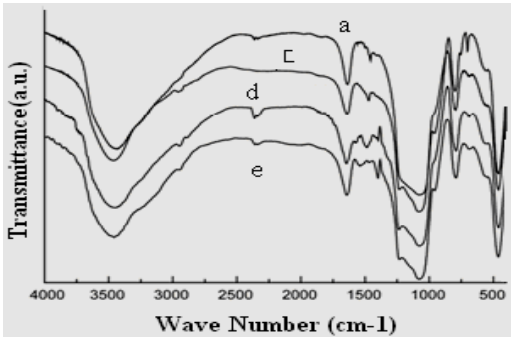

Fig. 6: FTIR spectrum of CFA-MCM-41 (a, c, d, e)

3.5 SEM-Analysis

The crystallite size and morphology of the calcined samples were determined by a scanning electron microscope (Model JEOL JSM 5200) equipped with energy dispersive X-ray analysis (EDAX).SEM images of CFA-MCM-41(b, d) are depicted in Fig.7 represents that the resulting particles are almost spherical in shape with no agglomerations. Small spherical particles are of CFA-MCM-41(d) with diameters of 85 to 235nm. It is observed that the average diameter of the

International Journal of Engineering, Science and Mathematics
Vol. 6 Issue 6, October 2017,
ISSN: 2320-0294 Impact Factor: 6.765
Journal Homepage: http://www.ijesm.co.in, Email: ijesmj@gmail.com Double-Blind Peer Reviewed
Refereed Open Access International Journal - Included in the International Serial Directories Indexed & Listed at: Ulrich's Periodicals Directory ©, U.S.A., Open J-Gage as well as in Cabell's Directories of Publishing Opportunities, U.S.A

particles is slightly increased as the synthesis temperature is raised from 30^0C to 160^0C after calcination. However when the synthesis temperature was around 130^0C, the prepared sample has indicated a good structural morphology.

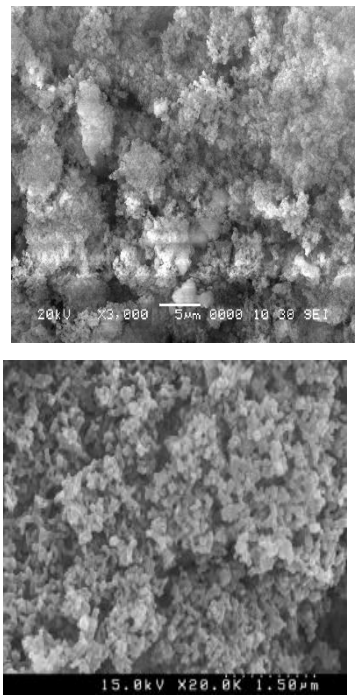

Fig. 7 SEM images of CFA-MCM-41(b, d)

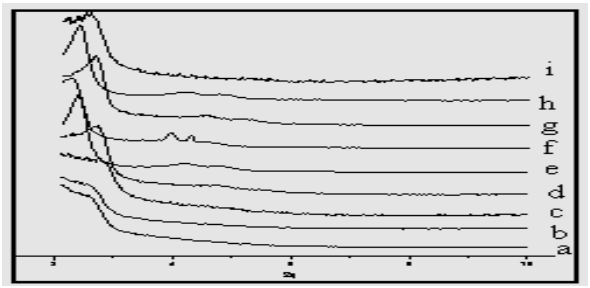

Fig.8 XRD patterns of calcined samples of CFA-MCM-41(a, b, c, d, e, f, g, h, i) at various pH of gel.

3.6 Influence of pH

To optimize the effect of pH as one of the synthesis parameter the gel was prepared at the different pH 1.87, 3.32, 4.72, 5.73, 6.25, 6.91, 8.56, 10.12 and 11.20, while other synthesis parameters values are kept constant

I) XRD-studies

The uniqueness of mesoporous structure, phase purity, degree of ordered ness and unit cell parameters of CFA-MCM-41 synthesized by varying pH of gel were determined from powder X-ray diffraction. Fig.8 demonstrates the XRD patterns of the calcined CFA-MCM-41 materials prepared from gels at different pH, which shows important differences in the long-range ordering and characteristic diffraction patterns of mesoporous materials. The well-defined XRD pattern of CFA-MCM-41 at pH 6.91 (f) can be indexed to the (100), (110), (200) and (210) and treated as 100 % crystalline

XRD pattern of the sample CFA-MCM-41 synthesized form highly alkaline gel (pH= 11.2) shows with only one prominent diffraction peak indicates a lamellar phase similar to a sample obtained from highly acidic gel. Hence it is concluded that to obtain well order MCM-41 phase the pH value is to be optimized for a given system. In the present molar scheme of synthesis, an optimized pH value is 6.91 (neutral). This result is

International Journal of Engineering, Science and Mathematics
Vol. 6 Issue 6, October 2017,
ISSN: 2320-0294 Impact Factor: 6.765
Journal Homepage: http://www.ijesm.co.in, Email: ijesmj@gmail.com Double-Blind Peer Reviewed
Refereed Open Access International Journal - Included in the International Serial Directories Indexed & Listed at: Ulrich's Periodicals Directory ©, U.S.A., Open J-Gage as well as in Cabell's Directories of Publishing Opportunities, U.S.A

in accordance with SEM analysis. However, a partial structural collapse of the material, arise from the inherent poor hydrothermal stability with respect to the pH of gel.

The well-ordered mesoporous structure of CFA-MCM-41(f) sample may be due to the simultaneous condensation of organic micelles, thereby influencing the unit cell parameters, wall thickness and the long-range ordering.

The summarized data for *d* spacing and unit cell values calculated from XRD patterns for different pH values presented in Table 3.Tabulated data represents slight shift of the characteristic peak at 100 to lower angle with a corresponding linear increase in *d* spacing and unit cell parameter as pH increases.

The X-ray diffraction data is further analyzed to estimate percent crystallinity of the samples obtained for different pH of gels. The obtained values of % crystallinity were further plotted as a function of pH of gel as shown in Fig.9. It is seen from the Fig.9 that up to pH=6.25 the rate of conversion of amorphous to crystallization of CFA-MCM-41 phase was slow as compare to 6.25 to 6.91 increase. Therefore, the rate of crystallization decreases as the process approaches to the completion indicated by constancy (100 %) in percent crystallization. Table 3 indicates that as pH varies from 1.87 to 11.20, unit cell parameter has been changed by 22.2 %

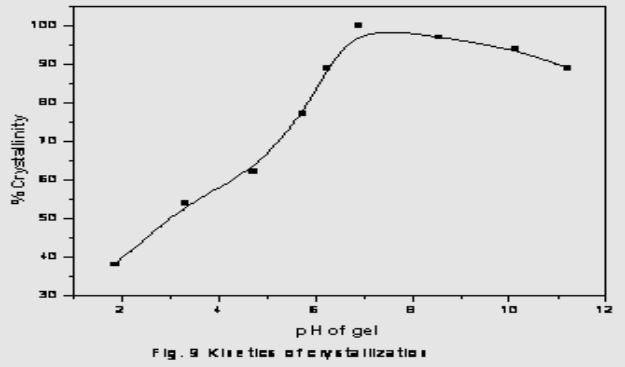

Fig. 9 Kinetics of crystallization

II) BET surface area and pore volume of CFA-MCM-41

The samples synthesized with different pH have also been characterized further by N_2-sorption studies. The isotherms of the selected samples for pH 5.73, 6.91, 8.56 and 11.20 are represented in Fig. 10 A,B. These isotherms are of type IV[19].

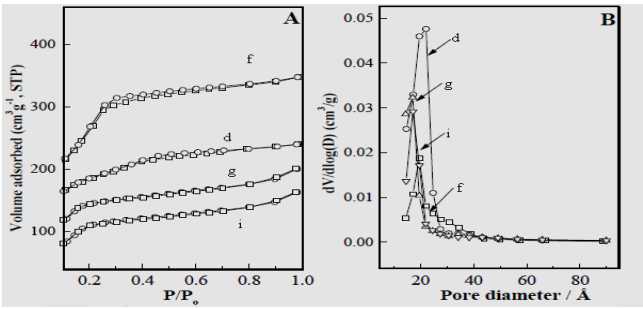

Fig. 10 (A) N2 adsorption-desorption isotherms and (B) pore size distribution of CFA-MCM-41(d, f, g, i)

International Journal of Engineering, Science and Mathematics
Vol. 6 Issue 6, October 2017,
ISSN: 2320-0294 Impact Factor: 6.765
Journal Homepage: http://www.ijesm.co.in, Email: ijesmj@gmail.com
Double-Blind Peer Reviewed
Refereed Open Access International Journal - Included in the International Serial Directories Indexed & Listed at: Ulrich's Periodicals Directory ©, U.S.A., Open J-Gage as well as in Cabell's Directories of Publishing Opportunities, U.S.A

Table 3 Effect of calcination temperature on Structural and textural properties of CFA-MCM-41

Sample name and pH of Gel	d100	Unit cell parameter	S.A. (m^2/g)	Average Pore diameter (Å)	Pore volume (ml/g)	Average wall thickness(Å)	% Crystallanity
CFA-MCM-41(a) P^H 1.87	30.87	35.50	_	_	_	_	38
CFA-MCM-41(b) P^H 3.32	32.94	37.88	588.13	32.14	0.567	5.74	54
CFA-MCM-41(c) P^H 4.72	33.19	38.17	863.27	31.84	0.688	6.33	62
CFA-MCM-41(d) P^H 5.73	33.31	38.31	970.32	29.46	0.879	8.85	77
CFA-MCM-41(e) P^H 6.25	33.56	38.79	_	_	_	_	89
CFA-MCM-41(f) P^H 6.91	33.95	39.04	1107.8	27.98	0.776	11.06	100
CFA-MCM-41(g) P^H 8.56	35.43	40.75	1000.7	29.91	_	10.84	97
CFA-MCM-41(h) P^H10.12	36.78	42.30	_	_	_	_	94
CFA-MCM-41(i) P^H11.20	37.72	43.38	467.13	33.19		10.19	89

Table 3 includes the numerical data for Surface Area, pore volume, pore diameter, and wall thickness as a result of N_2 sorption. Highest surface area was found for the sample with pH of 6.91. It is also revealed from the data, that as the pH value increases, surface area also increases[20] but when it declines to more basicity it gate drastically reduced from 1107.8 to 467.13m^2/g with subsidiary change in the average pore diameter and wall thickness this is because at high pH, solubility of silica increases rapidly due to which a higher amount of silica is left in the solution at the end of the synthesis. As the pH increases up to 6.91 the nucleation rate becomes higher forming smaller particles and higher surface area.

III) FTIR-studies for variation in Gel pH

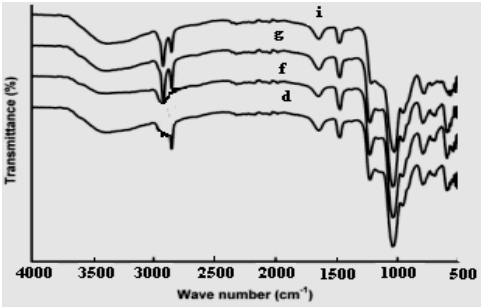

Fig. 11: FTIR spectrum of CFA-MCM-41 (d, f, g, i)

The FTIR spectra of calcined CFA-MCM-41(d, f, g, i) synthesized at gel pH 5.73, 6.91, 8.56 and 11.20 are illustrated in Fig.11. The broad band around3477.2cm^{-1}indicates the hydrophilicity of silica framework. The appearance of peaks at 2922.9cm^{-1} and 2852.5cm^{-1} for samples d, g, i can be concluded due to the effect of sulphate ions of H_2SO_4 during precipitation. However, the peak at 2923.2$cm^{-1}$is prominently found to be changed due to the effect of pH during synthesis. The effect observed for CFA-MCM-41(f) is significant, which is well supported by the XRD analysis and

International Journal of Engineering, Science and Mathematics
Vol. 6 Issue 6, October 2017,
ISSN: 2320-0294 Impact Factor: 6.765
Journal Homepage: http://www.ijesm.co.in, Email: ijesmj@gmail.com Double-Blind Peer Reviewed
Refereed Open Access International Journal - Included in the International Serial Directories Indexed & Listed at: Ulrich's Periodicals Directory ©, U.S.A., Open J-Gage as well as in Cabell's Directories of Publishing Opportunities, U.S.A

sorption studies of the samples. Rest of the peaks is the usual stretching for MCM-41.

V) SEM-Analysis

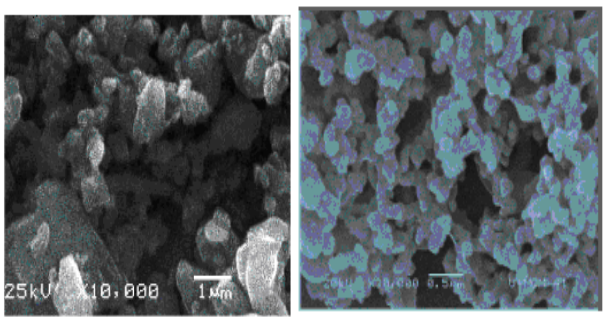

Fig.12 SEM images of CFA-MCM-41(f, i)

The morphology of the CFA-MCM-41 as a function of pH of gel was directly monitored by SEM as shown in fig.12. The SEM results indicate that the material surface starts to become rough and form nano-scale particles above pH 6.91 the nano-scale particles increases with further increasing pH. SEM images of CFA-MCM-41(f, i) are depicted in Fig.12 represents that the resulting particles are almost spherical in shape having diameters ranging from 21.0-140nm without agglomerations. It is observed that the average diameter of the particles is considerably altered as the pH is raised from 1.85 to 11.20. However when the pH of gel was around 6.91, the prepared sample indicated a good structural morphology.

3.7 CFA-MCM-41 at Optimized conditions Fig.13 shows the XRD pattern of optimized sample. The formation of three angle reflections 110,200,210 other than d_{100} indicates that the product possesses the symmetrical hexagonal pore structure typical of MCM-41. Fig.15 presents typical micrographs of synthesized CFA-MCM-41 samples. It exhibits uniform spherical shaped particles having small agglomerates with sizes between 30 and 200 nm. Fourier Transformed Infrared (FTIR) spectra of the final CFA-MCM-41 material can capitulate information concerning structural details as given below.

The adsorption/desorption isotherms of N_2 shown in Fig.15 and the values of specific BET surface area, mean pore diameter of the mesopores, pore volume and wall thickness obtained for fully crystalline CFA-MCM-41 are 1107.6 m^2/g ,26.38 Å, 0.879 ml/g and 17.95 Å respectively.

Thermo-gravimetric analysis of the final CFA-MCM-41 sample presented a TG/DTG curve as shown in Fig.16. The synthesized material presents approximately 50 wt% of the MCM-41 phase. The remaining part corresponds to organic material whose mass loss is related to three exothermal stages: (a) between 100-285 °C: decomposition of the surfactant2; (b) between 285-400 °C: breaking of the hydrocarbon chain, and (c) between 500-700 °C: combustion of the surfactant and water loss associated with condensation of silanol groups

International Journal of Engineering, Science and Mathematics
Vol. 6 Issue 6, October 2017,
ISSN: 2320-0294 Impact Factor: 6.765
Journal Homepage: http://www.ijesm.co.in, Email: ijesmj@gmail.com Double-Blind Peer Reviewed
Refereed Open Access International Journal - Included in the International Serial Directories Indexed & Listed at: Ulrich's Periodicals Directory ©, U.S.A., Open J-Gage as well as in Cabell's Directories of Publishing Opportunities, U.S.A

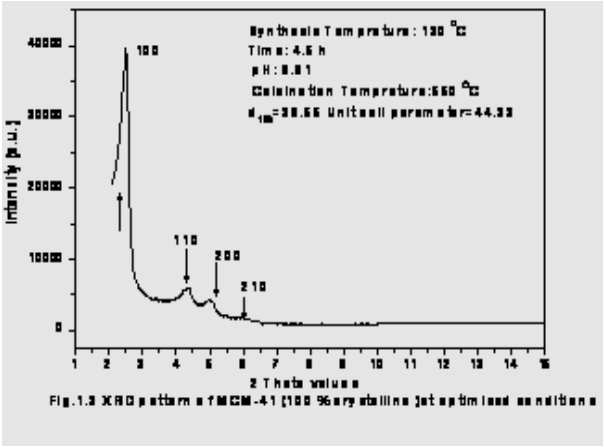

Fig.1.3 XRD pattern of MCM-41 (100 % crystallinity) at optimized conditions

Internal tetrahedral	**Asymmetric stretch 1250–950cm^{-1} ,Symmetric stretch720-650cm^{-1}**
External linkage	**Double ring 650–500cm^{-1} ,Pore opening 300-420cm^{-1} Symmetric stretch 750–820cm^{-1} ,Asymmetric stretch1050-1150cm^{-1}**

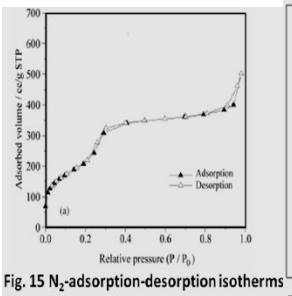

Fig. 15 N_2-adsorption-desorption isotherms CFA-MCM-41

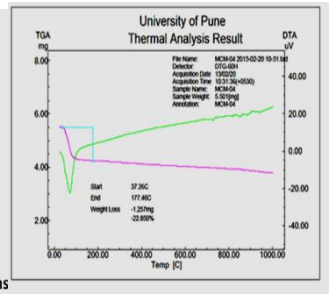

Fig.16 TGA-DTG analysis of the final CFA-MCM-41 sample.

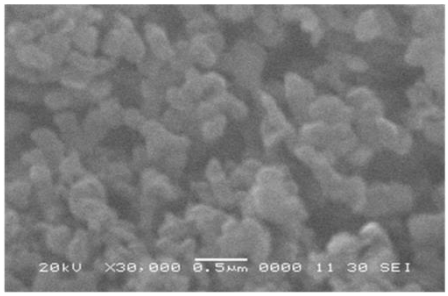

Fig.14: presents typical SEM synthesized CFA-MCM-41 of well orderd and fully crstalline

Conclusions:

Based upon the experimental study it was concluded that pure and well ordered CFA-MCM-41 material could be successfully synthesized from an industrial waste coal fly ash as the silica source instead of commercial expensive silica sources .The parametric variations such as change of synthesis temperature and pH of gel helps to optimize the synthesis conditions. The well ordered mesoporous material CFA-MCM-41 can be synthesized at 130^{0}C for 4h keeping pH of gel 6.91 and calcined at 550^{0}C.The apparent activation energy of conversion of synthesis gel to 100 % crystalline CFA-MCM-41 phase was 169.44 kJ/mole calculated by Arrhenius equation.

Refrences:

1. Carlson CL, Adriano DC Environmental impacts of coal combustion residues. *J Environ Qual* (1993)22:227–247
2. Forstner U Applied environmental geochemistry. *Academic Press, London*, (1983) p 395
3. Jones KC Contamination trends in soils and crops. *Environ Pollut*(1991) 69:311–325
4. Satyanarayana Raju MV Pollution status of soils near ash pond of a thermal power station (1993)
5. Coal demand and linkages 1994/95 to 1996/97 and 2001/02—midterm appraisal of *Eighth Five Year Plan*. August 1994.

6. Coal Directory of India, 1996–97. Calcutta: Ministry of Coal. *Coal Controller's Organization*, 1997, 128pp.
7. Fourth National Power Plan, 1997–2012. *Central Electricity Authority, Government of India*, 1997.
8. Narasimhan, K.S., Bhoumik, S.K., Reddy, P.S.R., Prakash, S., Biswal,S.K., 1997. Washability characteristics of Indian coals. *Journal of Mines,Metals and Fuels*.45,233–237.
9. Fox, C.S.,The Lower Gondwana coalfields of India: Calcutta, India, *Memoirs of the Geological Survey of India, v. LIX*, (1934)368 p.
10. Yanagisawa, Tsuneo; Shimizu, Toshio; Kuroda, Kazuyuki; Kato, Chuzo (1990). "The preparation of alkyltrimethylammonium-kanemite complexes and their conversion to microporous materials". *Bulletin of the Chemical Society of Japan* **63** (4): 988.
11. J. Rouquerol et al. (1994). "Recommendations for the characterization of porous solids " *Pure & Appl. Chem* **66** (8): 1739–1758.
12. J. S. Beck; J. C. Vartuli; W. J. Roth; M. E. Leonowicz; C. T. Kresge; K. D. Schmitt; C. T-W.Chu; D. H. Olson; E. W. Sheppard; S. B. McCullen; J. B. Higgins; and J. L. Schlenkert (1992). "A New Family of Mesoporous Molecular Sieves Prepared with Liquid Crystal Templates". *American Chemical Society* **114** (114): 10834–10843.
13. Brian Trewyn, et al. (2007). "Synthesis and Functionalization of a Mesoporous Silica Nanoparticle Based on the Sol–Gel Process and Applications in Controlled Release". *Accounts of Chemical Research* **40** (40): 846–853.
14. D.H. Park, C.-F. Cheng, H. He and J. Klinowski, *J. Mater. Chem*., 1997, 7(1),159-162.
15. K.M. Reddy, I. Moudrakovski and A. Sayari, *J. Chem. Soc., Chem. Commun*.,1994, 1059-1060.
16. J.S. Reddy and A. Sayari, J. *Chem. Soc., Chem. Commun*., 1995, 2231-2232.
17. F. Deng, R. A. Johnson, P. M. Asbeck, S. S. Law, W. B. Dubbelday, T. Hsiao, and J. Woo, SSalicidation process using NiSi and its device applications T, *J. Appl. Phys*. Vol. 81, p.8047, 1997.
18. Shiralkar, V.P. and Clearfield, A., *Zeolite*, 9, 363 (1989).
19. Gregg, S.J., and Sing, K.S.W., Adsorption, Surface Area and Porosity, *Academic Press London*, Ch. 4 (1982).
20. A. Corma, M.T. Navarro and J.P. Pérez-Pariente, *J. Chem. Soc., Chem.Commun*., 1994, 147-148.

****